PASSAGE OF SPHERICAL SHOCK WAVES THROUGH THERMALS

V. A. Andrushchenko

UDC 533.6.011.72

A study is made of the complex flow which develops in the passage of a shock
wave through a cloud of hot gas. Several new effects are discovered.

The problem of the propagation of shock waves in gas clouds with variable parameters
has recently been under intensive study in astrophysics, the theory of combustion, and plasma physics. The investigations [1, 2] experimentally examined the interaction of shock
waves with entropy discontinuities and looked at acoustic and dynamic aspects of the problem. Simple mathematical models were constructed for some of the effects observed. The
authors of [3, 4] studied the passage of shock waves through a weakly-ionized plasma cloud
from a laser spark. They examined the question of the dissipation of shock waves in the
hot region of the spark.

Here, we numerically study a two-dimensional axisymmetric problem on the interaction of
a spherical blast wave of volcanic origin with a hot eruptive cloud; some of the effects observed experimentally in [1-4] are confirmed and several new phenomena are discovered.

1. We will examine the problem of the passage of a spherical shock wave through a
cloud from a volcanic eruption. The cloud is modeled by a spherical thermal consisting of
nonuniformly heated gas. Here, we ignore the chemical composition of the cloud and its
content of suspended dust. It is assumed that the centers of the thermal and the explosion
are located on the same vertical at the initial moment of time. In the absence of lateral
perturbations (such as wind), motion is axisymmetric. As the mathematical model, we will
use the complete system of nonsteady Navier–Stokes equations for a compressible heat-conducting gas in the cylindrical coordinates r and z (see [5]). The gas is presumed to be perfect,
with the equation of state $p = A_\rho T$. The viscosity coefficient μ and thermal conductivity k
are assumed to be constant, while the atmospheric density $\rho_a(z)$ and pressure $p_a(z)$ decrease
exponentially with altitude z.

We seek to solve the initial equations in the region formed by the plane $z = 0$ (passing
through the center of the explosion), the symmetry axis $r = 0$, and the movable right $r =
f(t)$ and upper $z = \varphi(t)$ boundaries. The movable boundaries are located far enough from the
thermal and the shock front and move in such a way that the values of the gas dynamic parameters on the boundaries are equal to the corresponding parameters of the undisturbed surrounding medium, i.e., $r = f(t)$ and $z = \varphi(t)$: $u = v = 0$, $p = p_a(z)$, $T = T_a$. At $z = 0$, we impose
the boundary conditions: $v = \partial u/\partial z = \partial T/\partial z = 0$, while on the axis at $r = 0$ we impose the
symmetry conditions: $u = \partial v/\partial r = \partial p/\partial r = \partial T/\partial r = 0$.

In choosing the initial conditions, we use data on impulsive inversions of moderate intensity [6, 7]. Thus, the initial radii of the thermal and the spherical shock wave $R_0 =
50$ m, while the temperature in the cloud changes beginning with a certain point ($r = 0$, $z =
H_0$) by the law $T = T_a + (T_1 - T_a) \exp[-(4R/R_0)^2]$, $R = \sqrt{r^2 + (z - H^0)^2}$, $T_a = 288$ K, $T_1 = 2000$
K, $H^0 = 100$ m. The distribution of gas dynamic parameters inside the shock front corresponds to the solution of the problem of a spherical explosion at the point $r = 0$, $z = 0$ [8];
outside the front, the gas is at rest: $u = v = 0$, $p = p_a(z)$.

We introduce the following characteristic scales in the problem: $L = H^0 = 100$ m for
length; $\sqrt{L/g} = 3.2$ sec for time; $\sqrt{Lg} = 31$ m/sec for velocity; $T_a = 288$ K for temperature;
$\rho_0 = \rho_a(0) = 1.23$ kg/m³ for density. As a result of the conversion to dimensionless quantities, we obtain the following parameters for the problem: $Re = L\sqrt{Lg}\rho_0/\mu$, Reynolds number;
$Pr = \mu c_p/k$, Prandtl number; $M = \sqrt{Lg/\gamma A T_a}$, Mach number; $\gamma = c_p/c_v$, adiabatic exponent.
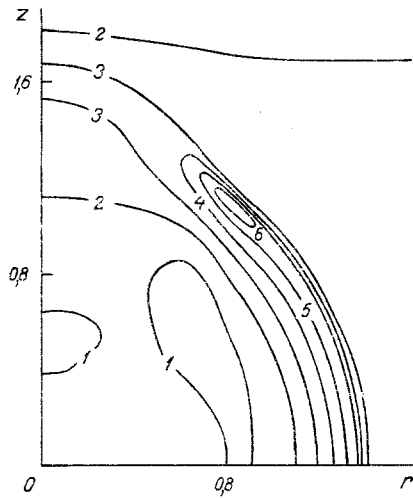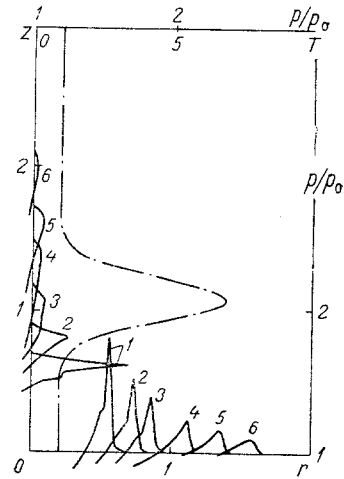
Fig. 1

Fig. 2

Fig. 1. Distribution of isobars for the moment of time t = 0.22 sec: 1) 0.93; 2) 0.98; 3) 1.03; 4) 1.08; 5) 1.13; 6) 1.18.

Fig. 2. Profiles of pressure on the coordinate axes for six moments of time: 1) 0.032 sec; 2) 0.064 sec; 3) 0.096 sec; 4) 0.16 sec; 5) 0.22 sec; 6) 0.32 sec.

In dimensionless variables, the initial system of equations has the form:

$$\frac{\partial u}{\partial t} + u\frac{\partial u}{\partial r} + v\frac{\partial u}{\partial z} = -\frac{1}{\gamma M^2 \rho}\frac{\partial p}{\partial r} + q_1,$$

$$\frac{\partial v}{\partial t} + u\frac{\partial v}{\partial r} + v\frac{\partial v}{\partial z} = -\frac{1}{\gamma M^2 \rho}\frac{\partial p}{\partial z} + q_2 + C_z,$$

$$\frac{\partial T}{\partial t} + u\frac{\partial T}{\partial r} + v\frac{\partial T}{\partial z} = -(\gamma - 1)T\,\mathrm{div}\,\mathbf{v} + (q_3 + Q)/\rho,$$

$$\frac{\partial p}{\partial t} + u\frac{\partial p}{\partial r} + v\frac{\partial p}{\partial z} = -\gamma p\,\mathrm{div}\,\mathbf{v} + q_3 + Q,$$

$$q_1 = \frac{1}{\mathrm{Re}\,\rho}\left\{-\frac{\partial}{\partial r}\left(\frac{2}{3}\mu\,\mathrm{div}\,\mathbf{v}\right) - \frac{2\mu u}{r^2} + \frac{2}{r}\frac{\partial}{\partial r}\left(\mu r\frac{\partial u}{\partial r}\right) + \right.$$
$$\left. + \frac{\partial}{\partial z}\left[\mu\left(\frac{\partial u}{\partial z} + \frac{\partial v}{\partial r}\right)\right]\right\}, \tag{1}$$

$$q_2 = \frac{1}{\mathrm{Re}\,\rho}\left\{-\frac{\partial}{\partial z}\left(\frac{2}{3}\mu\,\mathrm{div}\,\mathbf{v}\right) + \frac{1}{r}\frac{\partial}{\partial r}\left[r\mu\left(\frac{\partial u}{\partial z} + \frac{\partial v}{\partial r}\right)\right] + \right.$$
$$\left. + \frac{\partial}{\partial z}\left(2\mu\frac{\partial v}{\partial z}\right)\right\},$$

$$q_3 = \frac{(\gamma-1)\gamma M^2}{\mathrm{Re}}\mu\left\{2\left[\left(\frac{\partial u}{\partial r}\right)^2 + \left(\frac{\partial v}{\partial z}\right)^2 + \left(\frac{u}{r}\right)^2\right] + \right.$$
$$\left. + \left(\frac{\partial u}{\partial z} + \frac{\partial v}{\partial r}\right)^2 - \frac{2}{3}(\mathrm{div}\,\mathbf{v})^2\right\},$$

$$Q = \frac{\gamma}{\mathrm{Re}\,\mathrm{Pr}}\left[\frac{1}{r}\frac{\partial}{\partial r}\left(kr\frac{\partial T}{\partial r}\right) + \frac{\partial}{\partial z}\left(k\frac{\partial T}{\partial z}\right)\right].$$

The governing parameters of the problem were chosen as follows: Re = 50, M = 0.1, γ = 1.4, C_z = − 1.

System of differential equations (1) is approximated by means of an implicit difference scheme involving branching of the functions and coordinates and having second-order accuracy [9]. We use a through method of calculation. Since the chosen scheme is nonmonotonic, non-
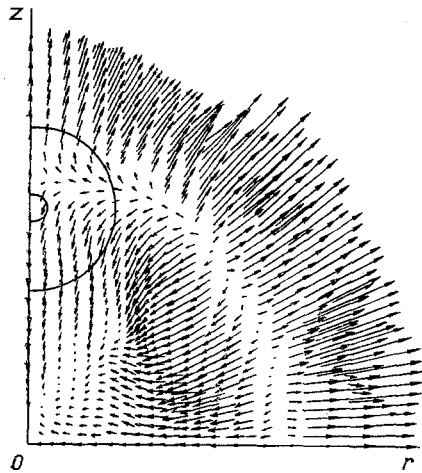
Fig. 3

Fig. 4

Fig. 3. Distribution of the velocity field at t = 0.32 sec.
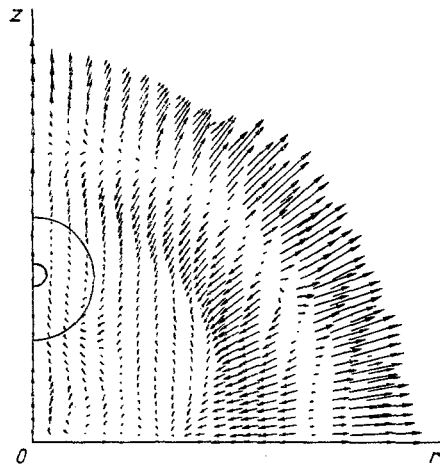
Fig. 4. Distribution of the velocity field at t = 0.45 sec.

physical oscillations develop with through calculation of the shock fronts. To damp these oscillations and reinforce the stabilizing properties of the scheme, we use smoothing operators. We use a "monotonizer" of the Buch—Boris type proposed in [10] and explicit linear three-point smoothing (see [8]).

The accuracy of the results is checked by varying the number of nodes of the theoretical grid and checking for satisfaction of the conservation laws. The relative errors for mass and energy are found as follows:

$$\delta M = (M_0 - M_1)/M_0, \quad \delta E = (E_0 - E_1)/E_0,$$

where

$$M_0 = 2\pi \int_0^l \int_0^\varphi \rho(r, z, 0)\, r\,dr\,dz, \quad M_1 = 2\pi \int_0^l \int_0^\varphi \rho(r, z, t)\, r\,dr\,dz;$$

$$E_0 = 2\pi \int_0^l \int_0^\varphi \varepsilon(r, z, 0)\, r\,dr\,dz, \quad E_1 = 2\pi \int_0^l \int_0^\varphi \varepsilon(r, z, t)\, r\,dr\,dz;$$

here, $\varepsilon = p/(\gamma - 1) + \gamma M^2 \rho(|v|^2/2 + z)$ is the total energy.

The calculation was performed on a 101 × 201 grid on an És-1055M computer.

2. Let us proceed to the analysis of the results. We are examining the situation when ejection of the volcanic cloud is followed by an explosion and the formation of a spherical shock wave that overtakes the cloud. We calculated two variants: with initial pressure gradients on the wave front $p_1/p_0 = 2.2$ and 1.5. However, since no qualitative differences were seen between these cases, we subsequently studied only the first case. The effects that were obtained were manifest to a somewhat greater degree in this instance.

A certain amount of time after the leading shock waves reaches the thermal, the part of the wave adjacent to the symmetry axis ends up in the body of the thermal and moves forward through heated gas. Since the velocity of perturbations is greater in hot gas than in an unheated medium, a section of the leading front in the cloud moves ahead of the remaining part of the front. Its accelerated motion eventually leads to its separation from the main front and the creation of a secondary structure in the form of a dome-shaped precursor.

Figure 1 shows the distribution of lines of equal pressure for the moment of time t = 0.22 sec. The isobar distribution clearly shows the movement of the precursor, with a maximum pressure on the leading edge equal to 1.03 versus a pressure of 1.13 for the main shock wave. Pressure drops sharply during passage through the hot cloud, and the distributions of the gas dynamic parameters become diffuse (see curves 1-3) in the horizontal and vertical directions (Fig. 2). Figure 2 shows the corresponding distributions of pressure on the axes

Or and Oz for several moments of time. The pressure profiles on the Or axis are identical to the profiles in the absence of a thermal. Here, the dot-dash line shows the distribution of temperature on the Oz axis. The distribution remains nearly unchanged during the time interval (0.032 sec; 0.32 sec). Thus, in the upper part of the front, the shock wave forms a "hole" — a low-pressure region through which the energy of the gas disturbed by the explosion begins to be pumped to the precursor. A similar phenomenon of "hole" formation in a shock front has been seen in experiments (see [3]) for the case of the passage of a weak spherical wave through a laser spark. The formation of a hole in this study was interpreted as the disappearance or dissipation of the shock wave (since it was remarked that recording techniques make it possible to fix the shock front in any case — even when its intensity has decreased by more than an order of magnitude). In fact, as the numerical experiment showed, the impossibility of locating the front can be explained by the following circumstance. During the formation of the precursor, the pressure profile turns out to be so diffuse that it can no longer be identified as a shock wave — not because of the low amplitude, but because of the relative length and the smallness of the gradients on the leading edge (see curves 3-4 in the horizontal and vertical directions in Fig. 2).

The energy transfer in the problem being examined here is more intensive than, for example, in the interaction of a shock wave with a thermal boundary layer (see [11]). Gas from the internal region and from zones near the leading edge adjacent to the precursor tends to move to the lower-density region near the symmetry axis and collapse about it, forming secondary detonational shock waves. One of these waves is directed upward and "feeds" the precursor. Propagating in the cloud, the precursor continuously increases in size and eventually embraces the entire flow region. Thus, the initial flow pattern is distorted. A second of the detonational shock waves creates an intensive flow in the form of a reactive jet in the neighborhood of the symmetry axis. This jet is directed downward (see the velocity field in the collapse region and below in Fig. 3; also shown in Fig. 3 are the external and internal boundaries of a thermal with temperatures of 425 and 1820 K, respectively). A similar reactive jet flowing downward has been seen in experiments (see [12]) in the study of the interaction of shock waves in air with a bubble of lighter gas.

One more feature of the flow being examined is the formation of a complex Mach configuration in the form of a suspended shock near the external boundary of the thermal (by approximately $t = 0.15$ sec). This shock arises from the collision of the precursor with the undisturbed front of the initial shock wave (see Fig. 1, where the isobar distribution clearly shows the suspended shock formed near the base of the precursor). As a result of this interaction, maximum pressures are realized in the region of the suspended shock. Thus, the pressure on this shock is 1.18 for the moment of time $i = 0.22$, while the pressure is 1.13 on the main front and 1.03 in the precursor.

Over time, the secondary detonational shock which is moving upward overtakes the leading edge of the precursor [and increases its amplitude somewhat as a result of the interaction (see curves 4 and 5 in the vertical direction in Fig. 2)]. Nevertheless, pressures are not subsequently equalized on the main front and in the precursor. By the moment of time $t = 0.32$ sec, pressure is equal to 1.1 on the shock front (on the Or axis), while it is equal to 1.02 on the leading edge (on the Oz axis) of the precursor — which has weakened in the acoustic medium.

The most intensive part of the leading front — which did not pass through the thermal — naturally propagates in the undisturbed atmosphere more rapidly than the precursor after the latter leaves the thermal. Over time, the external boundary of the gas that is moving first begins to take an ellipsoidal form (extended along the Oz axis). Then, roughly by the moment of time $t \approx 0.65$ sec, it begins to take a spherical shape. Although the radius of the leading edge increases by nearly a factor of six in this instance ($r_f \approx 280$ m), complete reestablishment of the shock wave does not take place — a "hole" remains in the top part of the front, while a suspended shock remains at the base of the precursor.

The numerical experiment also confirmed the observations made in [1] regarding the marked influence of a shock wave passing through a thermal on the dynamics of the latter. Interaction with the shock wave accelerates the process of vortex formation. A vortical develops in this case after 0.4 sec (see Fig. 4, which shows the distribution of the velocity field in the theoretical region for $t = 0.45$ sec; also shown are the external and internal boundaries of a thermal with the temperatures 425 and 1800 K), while a freely-rising thermal is transformed into a vortex ring roughly three times more slowly — over a time interval equal to 1-1.2 sec.

Interaction with a low-intensity spherical shock wave has little effect on the ascent of a thermal. The passage of the wave through the cloud lifts it slightly as a whole, while its hottest part is displaced upward somewhat relative to the center. Thus, by the moment of time t ≈ 0.65 sec, the thermal has risen 7 m in the case of interaction and 2 m in the case of free drift (the distance the thermal rose in these cases was determined from the hottest point). The difference between the results compared to the characteristic linear scales (50-100 m) is negligible.

In conclusion, we note that a check of the accuracy of the solution with regard to satisfaction of the conservation laws showed an error of 0.7% for mass and 2.1% for energy on a 101 × 210 grid. The results obtained on a double grid (201 × 401) were nearly the same as the main results.

LITERATURE CITED

1. R. P. Hamernik and D. S. Dosanjh, Phys. Fluids, 15, No. 7, 1248-1253 (1972).
2. F. V. Shugaev, Interaction of Shock Waves with Disturbances [in Russian], Moscow (1983).
3. E. M. Barkhudarov, V. R. Berezovskii, M. O. Mdivnishvili, et al., Pis'ma Zh. Tekh. Fiz., 10, No. 19, 1178-1181 (1984).
4. A. F. Aleksandrov, N. G. Vidyakin, V. A. Lakutin, et al., Zh. Tekh. Fiz., 56, No. 4, 771-774 (1986).
5. V. A. Andrushchenko, Kh. S. Kestenboim, and L. A. Chudov, Izv. Akad. Nauk SSSR Mekh. Zhidk. Gaza, No. 6, 144-151 (1981).
6. P. P. Firstov, P. I. Tokarev, and V. K. Lemzikov, Byull. Vulkanol. Stn. Akad. Nauk SSSR, No. 55, 151-157 (1978).
7. M. L. Asaturov, M. I. Budygo, K. Ya. Vinnikov, et al., Volcanoes, Stratospheric Aerosol, and the Earth's Climate [in Russian], Zemli, Leningrad (1986).
8. Kh. S. Kestenboim, G. S. Roslyakov, and L. A. Chudov, Point Explosion. Methods of Calculation. Tables, Moscow (1974).
9. V. I. Polezhaev, Some Applications of the Grid Method in Gas Dynamics [in Russian], Vol. 4, Moscow (1971), pp. 86-180.
10. A. I. Zhmakin and A. A. Fursenko, Zh. Vyschisl. Mat. Mat. Fiz., 20, No. 4, 1021-1031 (1980).
11. V. N. Gordeichik and I. V. Nemchinov, Applied Methods of Mechanics, Mosk. Fiz.-Tekh. Inst., Moscow (1983), No. 2529-84 Dep.
12. J. F. Haas and B. Sturtevant, Phys. Fluids, 29, No. 9, 2772 (1986).